

Intermediates Involved in the $2e^-/2H^+$ Reduction of CO_2 to CO by Iron(0) Porphyrin

Biswajit Mondal,[†] Atanu Rana,[†] Pritha Sen, and Abhishek Dey*

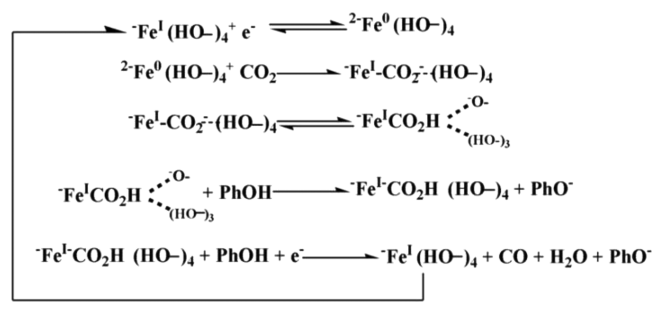
Department of Inorganic Chemistry, Indian Association for the Cultivation of Science, Kolkata 700032, India

S Supporting Information

ABSTRACT: The reduction of CO_2 by an iron porphyrin complex with a hydrogen bonding distal pocket involves at least two intermediates. The resonance Raman data of intermediate I, which could only be stabilized at $-95\text{ }^\circ\text{C}$, indicates that it is a $Fe(II)-CO_2^{2-}$ adduct and is followed by another intermediate II at $-80\text{ }^\circ\text{C}$ where the bound CO_2 in intermediate I is protonated to form a $Fe(II)-COOH$ species. While the initial protonation can be achieved using weak proton sources like MeOH and PhOH, the facile heterolytic cleavage of the C–OH bond in intermediate II requires strong acids.

Mitigation of CO_2 and assimilating it into useful chemicals is an urgent challenge in the context of growing concerns over the green house effect of CO_2 and depleting fossil fuels.^{1–4} Substantial focus is on the effective reduction of CO_2 into CO and other essential products.^{5–7} The direct reduction of CO_2 to $CO_2^{\bullet-}$ is highly energy demanding and occurs at fairly negative potential (-1.9 V vs SHE in acetonitrile).^{1,8,9} Kubiak et al. demonstrated the reduction of CO_2 to CO with Re-based molecular catalysts.^{10–12} They have further improved their catalyst by introducing a proton channel for enhancing the kinetics of the CO_2 reduction process.^{10,13,14} Sauvage used Nicylam and heme complexes for the reduction of CO_2 to CO in the 1980s.¹⁵ Saveant investigated the electrochemistry of CO_2 reduction with Fe porphyrin in detail^{16,17} and has modified this approach of CO_2 reduction by Fe porphyrin, with the iron in its formal zerovalent state, with the incorporation of a weak proton donor (like phenol) appended to the periphery of the porphyrin macrocycle to act as a proton relay during CO_2 reduction and thereby increasing the efficiency of the catalyst.^{4,18–21} By analyzing the electrocatalytic response, a plausible mechanism for the reduction of CO_2 by Fe(0) porphyrin was offered. CO_2 binds an Fe(0) center and upon subsequent proton and electron transfer, CO is released (Scheme 1). It was proposed that a concerted proton–electron transfer bond cleavage (CPETBC: electron transfer from the central atom concerted with proton transfer and breaking of one C–O bond) of a $Fe-COOH$ intermediate species is the rate-determining step in organic solvents. However, until date, no such intermediate has been isolated and spectroscopically characterized. Vibrational spectroscopy can be used to characterize the $M-CO_2$ adducts. The C–O vibrations are intense in the FTIR, and Kubiak has used *in situ* FTIR to show the formation of $[M-Ligand-CO]$ and $[M-Ligand-CO_2OH]$ as the end product of CO_2 reduction.²² Peters et al. also characterized a cobalt bound CO_2 adduct with FTIR.²³

Scheme 1. Proposed Mechanism of CO_2 Reduction to CO with Fe–Porphyrins



Over the last few years iron porphyrins that facilitate H-bonding in the distal pocket through triazoles have been reported.²⁴ This hydrogen bonding interaction has been demonstrated to increase the rate and selectivity of O_2 reduction by stabilizing intermediates involved in the process.²⁴ In this communication, two intermediates involved in the reduction of CO_2 to CO by Fe(0) porphyrins, which are stabilized by second sphere H-bonding pocket of the porphyrin ligand, are trapped at cryogenic temperatures and characterized using vibrational spectroscopy. Isotopic labeling of CO_2 by ^{13}C indicates the presence of Fe–C bonds in both. The role of proton source is evaluated using MeOH, PhOH, and *p*- $\text{CH}_3\text{C}_6\text{H}_4\text{SO}_3\text{H}$. The results indicate that the heterolytic cleavage of a C–OH bond in a $Fe^{II}-COOH$ intermediate is rate determining under these conditions.

CO_2 binds Fe–porphyrin complexes in its Fe(0) state as proposed by Saveant et al. Accordingly, in acetonitrile solvent, electroreduction of CO_2 is observed with $FeEs_4$ (Figure 1A). The potential of CO_2 reduction indicates that the formal Fe(0) oxidation state (Figure 1B) is the catalytically active species. Iron porphyrin with Fe(0) can be obtained, in solution, by the chemical reduction of Fe(III) porphyrin with sodium anthracene.^{25–28} The crystal structure of this dark green species shows an intact porphyrin macrocycle. In our pursuit, we used Na–Hg in THF–MeOH solution for the reduction of the $FeEs_4$ to its formal Fe(0) oxidation state and obtained a dark green solution, which is spectroscopically identical to that obtained using sodium anthracene (regeneration of the Fe(III) porphyrin took 3 equiv of ferrocenium; Figure S2). Upon bubbling CO_2 in the solution of Fe(0), the green color changes to red and the Soret band at 439 nm shifts to 421 nm (Figure S1, red) indicating the oxidation of Fe(0) porphyrin by CO_2 . The resonance Raman

Received: June 9, 2015

Published: August 20, 2015

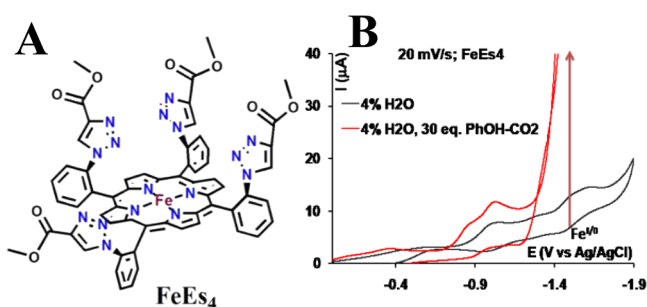


Figure 1. (A) Schematic representation of the complex. (B) Cyclic voltammogram of FeEs_4 in 4% H_2O containing acetonitrile (black) vs catalytic CO_2 reduction of same using 30 equiv of PhOH-CO_2 in 4% H_2O /acetonitrile mixture (red).

(rR) spectroscopy of the Fe(0)Es_4 shows a ν_4 band at 1325 cm^{-1} and 1336 cm^{-1} (Figure 2A, blue) and ν_2 band at 1542 cm^{-1} . The

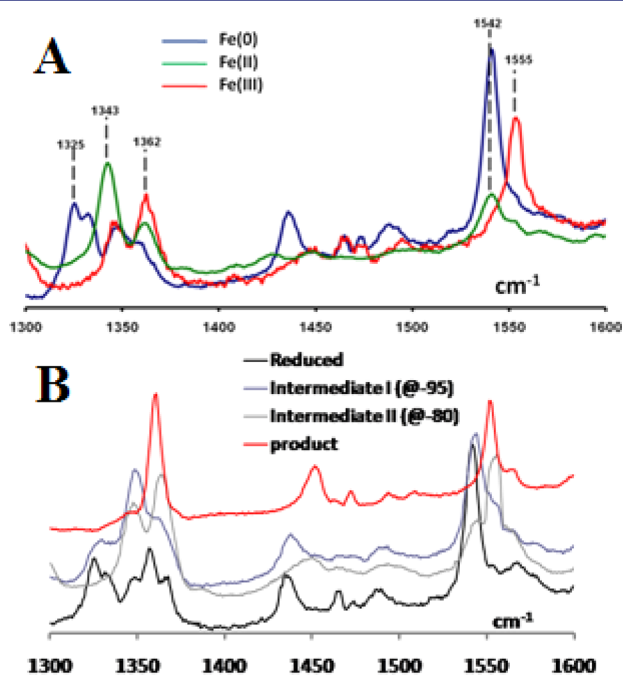


Figure 2. (A) Oxidation and spin state markers for Fe(III) (red), Fe(II) (green), and Fe(0) (blue). (B) Oxidation and spin state markers for Fe(0) (black), intermediate I (purple), intermediate II (gray), and product (red).

rR features of the species is different from those of Fe(III) (ν_4 at 1362 cm^{-1} ; ν_2 at 1555 cm^{-1}) and Fe(II) (ν_4 at 1342 cm^{-1} ; ν_2 at 1542 cm^{-1}) porphyrins (Figure 2A, red). On passing CO_2 over a Fe(0) solution at $-95\text{ }^\circ\text{C}$, a transient intermediate is observed ($t_{1/2} < 30\text{ s}$) with a new set of ν_4 and ν_2 vibrations at 1348 and 1544 cm^{-1} , respectively (intermediate I) (Figure 2B, blue). When the same solution is warmed up to $-80\text{ }^\circ\text{C}$ the ν_4 and ν_2 bands further shift to 1363 and 1555 cm^{-1} , respectively, suggesting the transition of intermediate I to a new intermediate (intermediate II) (Figure 2B, gray). This intermediate could be a protonated form of intermediate I (the solution contains MeOH as proton source). This proposition is inspired by the fact that, when a slightly more acidic proton source like PhOH is used, intermediate II is obtained even at $-95\text{ }^\circ\text{C}$ (Figure S3) and not intermediate I. Alternatively, when $p\text{-CH}_3\text{C}_6\text{H}_4\text{SO}_3\text{H}$ (PTSA) is

used as the proton source, the product ($\text{Fe}^{\text{II}}\text{-CO}$) is formed even at these low temperatures (*vide infra*).

The low frequency region of the rR spectra of the intermediate I, characterized by the unique set of ν_4 and ν_2 vibrations at 1348 and 1544 cm^{-1} , respectively, shows two sets of $^{13}\text{C}/^{12}\text{C}$ isotope sensitive bands. A very weak vibration appears at 590 cm^{-1} when $^{12}\text{CO}_2$ is used and shifts to 568 cm^{-1} upon using $^{13}\text{CO}_2$. Another vibration observed at 806 cm^{-1} with $^{12}\text{CO}_2$ shifts to 742 cm^{-1} on using $^{13}\text{CO}_2$ (Figure 3A). In the low frequency region of the rR

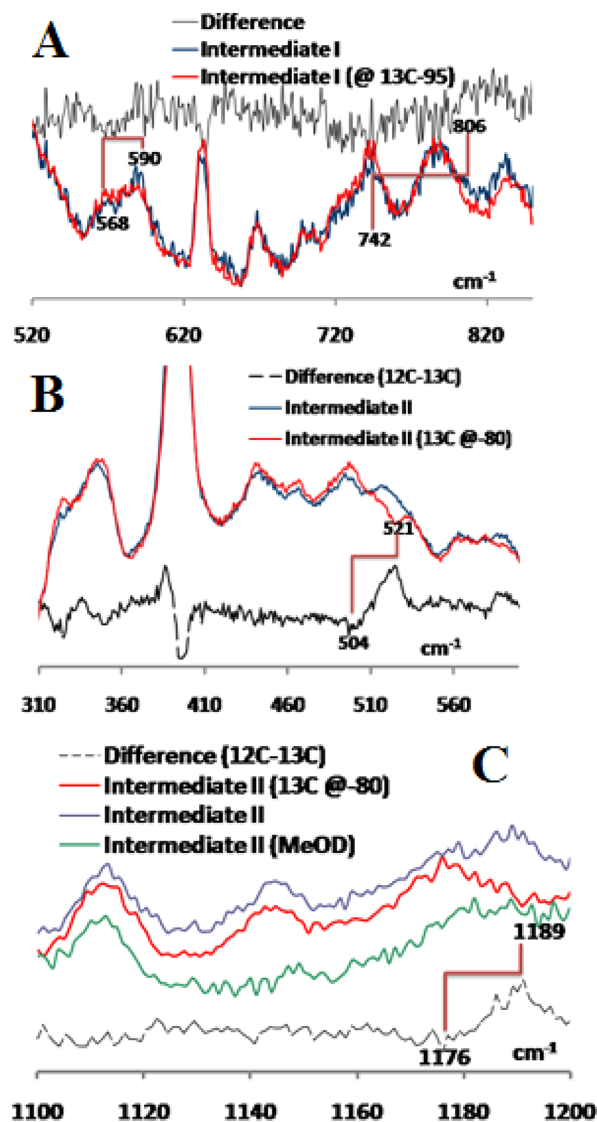


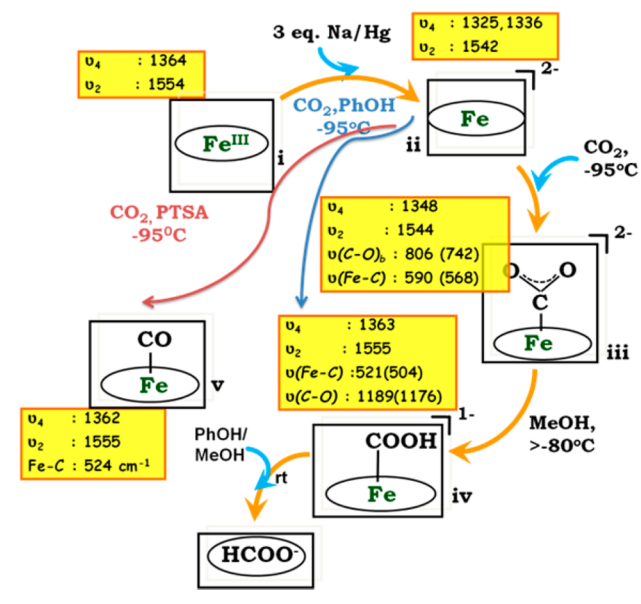
Figure 3. (A) Fe-C vibration of intermediate I at 590 cm^{-1} with $^{12}\text{CO}_2$ (blue) and its shift with $^{13}\text{CO}_2$ (red). (B) Fe-C vibration of intermediate II at 521 cm^{-1} with $^{12}\text{CO}_2$ (blue) and its shift with $^{13}\text{CO}_2$ (red). (C) C-OH vibration of intermediate II at 1188 cm^{-1} with $^{12}\text{CO}_2$ and its shift with $^{13}\text{CO}_2$ and deuteration.

spectra of the intermediate II, a band at 521 cm^{-1} shifts to 504 cm^{-1} upon $^{13}\text{CO}_2$ substitution (Figure 3B). Another vibration at 1188 cm^{-1} shifts to 1176 cm^{-1} upon $^{13}\text{CO}_2$ substitution (Figure 3C). When CD_3OD is used instead of MeOH as a proton source, the vibration at 1189 cm^{-1} disappears (Figure 3C, green). The same $^{12}\text{C}/^{13}\text{C}$ isotope shift for intermediate II is obtained when trapped at $-95\text{ }^\circ\text{C}$ in the presence of PhOH (Figure S3).

Thus, the observation of two intermediates, with vibrations between 500 and 600 cm^{-1} , sensitive to ^{13}C substitution of CO_2 , indicates that both of these intermediates bear Fe–C bonds. The ^{13}C sensitive band at 590 cm^{-1} of intermediate I likely represents a Fe–C stretch originating from a Fe– CO_2 adduct. It is possible that this mode will have contribution from intraligand modes of CO_2 . The vibration at 806 cm^{-1} likely represents a bending motion of the bound CO_2 . Similarly, the ^{13}C sensitive mode at 521 cm^{-1} in intermediate II is a Fe–C vibration originating from a Fe–COOH species, which results from protonating the Fe– CO_2 intermediate I. The mode at 1188 cm^{-1} is likely to be a bending mode of the bound carboxylate unit as indicated by its sensitivity to both ^{13}C and D substitution. The fact that the intermediate I is not obtained in the presence of PhOH is consistent with the above proposal. The intermediate II has a lifetime of ~ 1 – 2 min at room temperature, which allows detection of a carbonyl stretch at 1573 cm^{-1} and shifts to 1567 cm^{-1} when MeOD is used instead of MeOH in FTIR in addition to the formate with a carbonyl stretch at 1632 cm^{-1} formed by the solvolysis of the bound carboxylate group at elevated temperatures (Figure S4).

Based on the experimental data obtained here a mechanistic scheme can be proposed for the reduction of CO_2 by Fe(0) porphyrins in organic solutions. CO_2 binds Fe(0) porphyrin, and the Fe– CO_2 adduct (iii, Scheme 2) is characterized by Fe–C

Scheme 2. Mechanism of CO_2 Reduction to CO with FeEs₄



vibration at 590 cm^{-1} and CO bending mode at 806 cm^{-1} , which are both sensitive to ^{13}C substitution. This species has a very high pK_a as it is protonated easily by MeOH even at -80°C and could only be observed at -95°C . In the presence of PhOH, this could not be observed even at -95°C , and the protonated species (IV, Scheme 2) was observed instead. This protonated species shows a ^{13}C sensitive Fe–C vibration at 521 cm^{-1} and $^{12}\text{C}/^{13}\text{C}$ and H/D sensitive C–OH vibration at 1189 cm^{-1} . The fact that the protonation of intermediate I to form intermediate II can be achieved by MeOH implies that intermediate I is very basic and has a high pK_a . Intermediate II, however, offers Fe(II)–CO (i.e., the C–OH unit cleavage product) only in the presence of PTSA (Figure 4). In the absence of PTSA the intermediate II is hydrolyzed to generate formate (likely sodium formate,

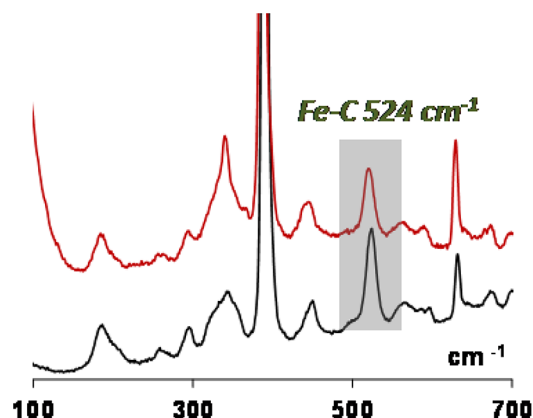


Figure 4. Fe–C stretch of the product ferrous carbonyl (red, product; black, pure Fe(II)–CO adduct).

HCOONa 1632 cm^{-1} , DCOONa 1626 cm^{-1} , Figure S4). Thus, the protonation of intermediate II resulting in the cleavage of the C–OH bond is likely to be the rds of the reaction. During electrochemical reduction of CO_2 by Fe(0) porphyrin, the rds was proposed to be a CPETBC to a FeCOOH species. Considering the fact that a FeCOOH species is found to be stable in the presence of PhOH, the same proton source used in the electrochemical study, it is reasonable that this species needs to be reduced, thereby increasing its electron density and enhancing the pK_a of the bound –COOH species, for PhOH to affect C–OH bond cleavage. Alternatively under single turnover conditions, a stronger acid like PTSA could cleave the C–OH bond of the Fe^{II}–COOH intermediate II without its further reduction.

The ν_4 and ν_2 vibrations have been found to be a reliable measure of oxidation states of Fe in iron–porphyrin complexes. The ν_4 and ν_2 of the Fe– CO_2 adduct are very similar to those reported for high spin Fe(II) porphyrins, indicating that this species is best described as a HS Fe^{II}– CO_2^{2-} species. The anionic state is likely stabilized by the hydrogen bonding distal site present in the FeEs₄ complex. Similar hydrogen bonding was experimentally observed in dioxygen adduct of the same complex. Consistently, no CO_2 bound intermediate (either iii or iv in Scheme 2) could be stabilized in FeTPP where the distal hydrogen bonding network is absent. The ν_4 and ν_2 vibrations of the intermediate iv in Scheme 2 are similar to that of the $S = 0$ Fe(II)–CO adduct where there is significant charge transfer from the Fe(II) to the CO π^* orbitals via backbonding. Thus, intermediate II is best described as a $S = 0$ Fe(II)–COOH species. Backbonding from Fe(II) to acyl π^* has been experimentally and theoretically demonstrated in the active site of mononuclear iron enzyme Hmd (H_2 -forming methylenetetrahydromethanopterin dehydrogenase) and its synthetic model complexes.^{29,30}

Density functional theory (DFT) calculations (Gaussian 03, BP86 functional)^{31–33} have been performed to obtain theoretical models for these CO_2 adducts stabilized by H-bonding. H-bonding is modeled using explicit water molecules (water molecules are trapped inside this triazole cavity).²⁴ The optimized structure of these adducts indicate (Figure 5) that the Fe–C bond vibrations are 687 cm^{-1} for intermediate I, which is lowered to 653 cm^{-1} for intermediate II. Intermediate I bears a high spin character with the ν_4 and ν_2 vibrations at 1337 and 1529 cm^{-1} , respectively, whereas intermediate II bears a low spin character with ν_4 and ν_2 bands at 1343 and 1573 cm^{-1} ,

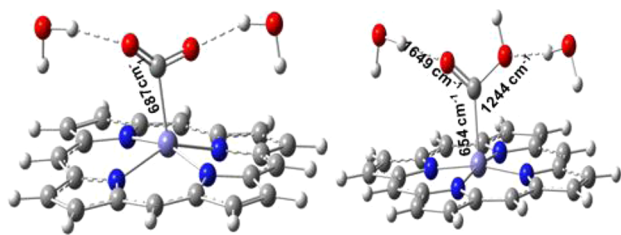


Figure 5. DFT optimized structures of Fe–CO₂ (intermediate I, left) Fe–CO₂H (intermediate II, right).

respectively. While the absolute values of the calculated frequencies are different from the experimental values, the lowering of Fe–C bond vibration and the shift of the ν_4 and ν_2 bands to higher wavenumbers from intermediate I to intermediate II are qualitatively in agreement with the experimental results (Table S1).

In conclusion, two intermediates involved in the reduction of CO₂ by Fe(0) porphyrins were trapped and characterized using rR spectroscopy. Based on the experimental data and DFT calculations it is proposed that an initial Fe^{II}–CO₂²⁻ adduct is protonated by a weak acid leading to the formation of a Fe^{II}–COOH species, which is then protonated by a stronger acid to eliminate H₂O and form the product Fe^{II}–CO. These intermediates can only be stabilized by the second sphere H-bonding interaction with the triazole groups in the distal side of the iron porphyrin.

■ ASSOCIATED CONTENT

📄 Supporting Information

The Supporting Information is available free of charge on the ACS Publications website at DOI: 10.1021/jacs.5b05992.

Detailed experimental protocols, additional spectroscopic data, and optimized coordinates (PDF)

■ AUTHOR INFORMATION

Corresponding Author

*icad@iacs.res.in

Author Contributions

[†]These authors contributed equally to this work.

Notes

The authors declare no competing financial interest.

■ ACKNOWLEDGMENTS

The research was funded by DST India (SB/S1/IC-25/2013). A.R. acknowledges Int. Ph.D. program of IACS, and B.M. and P.S. acknowledge CSIR-SPM-SRF and CSIR-JRF, respectively. We acknowledge Subhra Samanta and Kaustuv Mittra for their generous help in synthesis.

■ REFERENCES

- (1) Costentin, C.; Robert, M.; Saveant, J.-M. *Chem. Soc. Rev.* **2013**, *42*, 2423.
- (2) Elgrishi, N.; Chambers, M. B.; Fontecave, M. *Chem. Sci.* **2015**, *6*, 2522.
- (3) Clark, M. L.; Grice, K. A.; Moore, C. E.; Rheingold, A. L.; Kubiak, C. P. *Chem. Sci.* **2014**, *5*, 1894.
- (4) Costentin, C.; Drouet, S.; Passard, G.; Robert, M.; Savéant, J.-M. *J. Am. Chem. Soc.* **2013**, *135*, 9023.
- (5) Saouma, C. T.; Lu, C. C.; Day, M. W.; Peters, J. C. *Chem. Sci.* **2013**, *4*, 4042.
- (6) Fong, H.; Peters, J. C. *Inorg. Chem.* **2015**, *54*, 5124–5135.

- (7) Fujita, E. *Coord. Chem. Rev.* **1999**, *185–186*, 373.
- (8) Lamy, E.; Nadjro, L.; Saveant, J. M. *J. Electroanal. Chem. Interfacial Electrochem.* **1977**, *78*, 403.
- (9) Schwarz, H. A.; Dodson, R. W. *J. Phys. Chem.* **1989**, *93*, 409.
- (10) Machan, C. W.; Chabolla, S. A.; Yin, J.; Gilson, M. K.; Tezcan, F. A.; Kubiak, C. P. *J. Am. Chem. Soc.* **2014**, *136*, 14598.
- (11) Riplinger, C.; Sampson, M. D.; Ritzmann, A. M.; Kubiak, C. P.; Carter, E. A. *J. Am. Chem. Soc.* **2014**, *136*, 16285.
- (12) Vollmer, M. V.; Machan, C. W.; Clark, M. L.; Antholine, W. E.; Agarwal, J.; Iii, H. F. S.; Kubiak, C. P.; Walensky, J. R. *Organometallics* **2015**, *34*, 3.
- (13) Hawecker, J.; Lehn, J.-M.; Ziessel, R. *J. Chem. Soc., Chem. Commun.* **1984**, 328.
- (14) Wong, K.-Y.; Chung, W.-H.; Lau, C.-P. *J. Electroanal. Chem.* **1998**, *453*, 161.
- (15) Collin, J. P.; Sauvage, J. P. *Coord. Chem. Rev.* **1989**, *93*, 245.
- (16) Hammouche, M.; Lexa, D.; Savéant, J. M.; Momenteau, M. *J. Electroanal. Chem. Interfacial Electrochem.* **1988**, *249*, 347.
- (17) Hammouche, M.; Lexa, D.; Momenteau, M.; Saveant, J. M. *J. Am. Chem. Soc.* **1991**, *113*, 8455.
- (18) Costentin, C.; Drouet, S.; Robert, M.; Savéant, J.-M. *Science* **2012**, *338*, 90.
- (19) Costentin, C.; Passard, G.; Robert, M.; Savéant, J.-M. *J. Am. Chem. Soc.* **2014**, *136*, 11821.
- (20) Costentin, C.; Passard, G.; Robert, M.; Savéant, J.-M. *Proc. Natl. Acad. Sci. U. S. A.* **2014**, *111*, 14990.
- (21) Bhugun, I.; Lexa, D.; Saveant, J.-M. *J. Am. Chem. Soc.* **1994**, *116*, 5015.
- (22) Froehlich, J. D.; Kubiak, C. P. *J. Am. Chem. Soc.* **2015**, *137*, 3565.
- (23) Zhang, M.; El-Roz, M.; Frei, H.; Mendoza-Cortes, J. L.; Head-Gordon, M.; Lacy, D. C.; Peters, J. C. *J. Phys. Chem. C* **2015**, *119*, 4645.
- (24) Samanta, S.; Sengupta, K.; Mittra, K.; Bandyopadhyay, S.; Dey, A. *Chem. Commun.* **2012**, *48*, 7631.
- (25) Mashiko, T.; Reed, C. A.; Haller, K. J.; Scheidt, W. R. *Inorg. Chem.* **1984**, *23*, 3192.
- (26) Yamaguchi, K.; Morishima, I. *Inorg. Chem.* **1992**, *31*, 3216.
- (27) Dhanasekaran, T.; Grodkowski, J.; Neta, P.; Hambright, P.; Fujita, E. *J. Phys. Chem. A* **1999**, *103*, 7742.
- (28) Grodkowski, J.; Neta, P.; Fujita, E.; Mahammed, A.; Simkhovich, L.; Gross, Z. *J. Phys. Chem. A* **2002**, *106*, 4772.
- (29) Dey, A. *J. Am. Chem. Soc.* **2010**, *132*, 13892.
- (30) Dey, S.; Das, P. K.; Dey, A. *Coord. Chem. Rev.* **2013**, *257*, 42.
- (31) Becke, A. D. *Phys. Rev. A: At., Mol., Opt. Phys.* **1988**, *38*, 3098.
- (32) Perdew, J. P. *Phys. Rev. B: Condens. Matter Mater. Phys.* **1986**, *33*, 8822.
- (33) Frisch, M. J.; et al. *Gaussian 03*; Gaussian, Inc.: Wallingford, CT, 2004.